JOURNAL OF BACTERIOLOGY, Feb. 2004, p. 919–927 Vol. 186, No. 4
0021-9193/04/$08.00+0 DOI: 10.1128/JB.186.4.919–927.2004

Dynamics of Fruiting Body Morphogenesis

Dale Kaiser* and Roy Welch†

Departments of Biochemistry and Developmental Biology, Stanford University, Stanford, California 94305

Received 18 June 2003/Accepted 4 November 2003

Myxobacteria build their species-specific fruiting bodies by cell movement and then differentiate spores in specific places within that multicellular structure. New steps in the developmental aggregation of *Myxococcus xanthus* were discovered through a frame-by-frame analysis of a motion picture. The formation and fate of 18 aggregates were captured in the time-lapse movie. Still photographs of 600 other aggregates were also analyzed. *M. xanthus* has two engines that propel the gliding of its rod-shaped cells: slime-secreting jets at the rear and retractile pili at the front. The earliest aggregates are stationary masses of cells that look like three-dimensional traffic jams. We propose a model in which both engines stall as the cells' forward progress is blocked by other cells in the traffic jam. We also propose that these blockades are eventually circumvented by the cell's capacity to turn, which is facilitated by the push of slime secretion at the rear of each cell and by the flexibility of the myxobacterial cell wall. Turning by many cells would transform a traffic jam into an elliptical mound, in which the cells are streaming in closed orbits. Pairs of adjacent mounds are observed to coalesce into single larger mounds, probably reflecting the fusion of orbits in the adjacent mounds. Although fruiting bodies are relatively large structures that contain 10^5 cells, no long-range interactions between cells were evident. For aggregation, *M. xanthus* appears to use local interactions between its cells.

Myxobacteria build fruiting bodies that have a wide variety of shapes, each serving to differentiate 1 of the approximately 40 different myxobacterial species (25). Cylindrical and spherical masses of cells constitute the stalks, branches, and sporangioles (packages of myxospores) of these fruiting bodies. Although the shapes are relatively simple, they represent inherited patterns of cell movement. Their heritability over a billion years of speciation is demonstrated by the strong correlation between the morphology of fruiting bodies and their molecular phylogeny based on comparing 16S RNA sequences in these members of the delta subgroup of proteobacteria (36). Fruiting body development is initiated by starvation, and the structures are built entirely by cell movement. There is little cell division because starvation has induced the cells to give a stringent response; *Myxococcus xanthus* responds to starvation by arresting ribosome biosynthesis (8), by expressing a subset of its genes (20), and by adopting appropriate new patterns of cell movement (15). We sought to define these movement patterns and their role in building a fruiting body.

A new understanding of the mechanics of gliding motility and of its regulation in *M. xanthus* provided the starting point for the present investigation. *Myxococcus* cells, which are 5 to 7 μm long and 0.5 μm in diameter, glide over a surface, leaving behind a trail of slime (3, 5, 37). Hodgkin discovered that *M. xanthus* has two gliding engines encoded by nonoverlapping sets of genes (9). One engine is now considered to be an array of jets that are located at both ends of the cell and that secrete slime from one end at a time (41). The other engine is a polar cluster of retractile type IV pili located at one end of the cell (16, 38, 21). Using both engines, *M. xanthus* glides in one direction for a while and then reverses. A reversal is not accomplished by making a U-turn but by exchanging head for tail, as shown in a movie by L. Jelsbak attached to reference 15. Studies of *frz* mutants have revealed a cytoplasmic chemosensory pathway that can alter the probability of reversing direction (2). Kinetic measurements of swarm expansion show that the two engines most often cooperate in moving the cell (17). Cooperation strongly suggests that the two engines are switched from pole to pole by a tightly regulated and concerted mechanism. Individually, slime secretion (known as A motility) and pilus retraction (known as S motility) endow the cells with different swarm patterns, which combine in A^+S^+ cells (9). Both engines are needed for development because A^-S^- mutants cannot build fruiting bodies (9). Nevertheless, most A^-S^+ and A^+S^- strains are able to build fruiting bodies, although they build more slowly than A^+S^+ (Y. Cheng and D. Kaiser, unpublished observations). Although either engine is sufficient, this finding suggests that the coordination mechanism, which was intact in all of the A^-S^+ and A^+S^- strains tested, plays a role in development.

Wireman and Dworkin showed that *M. xanthus* and the closely related *M. fulvus* construct spherical fruiting bodies raised on a short stalk (recent isolates from soil) or raised mounds (domesticated laboratory strains) and then sporulate (40). Reichenbach et al. made a remarkable series of time lapse movies that compare the fruiting body development of different species (26–29). These films show that *Stigmatella* and *Chondromyces* spp., whose fruiting bodies have multiple sporangioles raised on a thick stalk, begin just like *M. xanthus* by raising a mound. Peripheral cells of *M. xanthus*, located outside but immediately adjacent to the mound, do not differentiate into spores (23). As a consequence only mound cells sporulate (14, 30). The developmental data raise the question of how *M. xanthus* regulates its movement so as to build a mound and

* Corresponding author. Mailing address: Departments of Biochemistry and Developmental Biology, Stanford University, Stanford, CA 94305. Phone: (650) 723-6165. Fax: (650) 725-7739. E-mail: kaiser@cmgm.stanford.edu.

† Present address: Biology Department, Syracuse University, Syracuse, NY 13244.

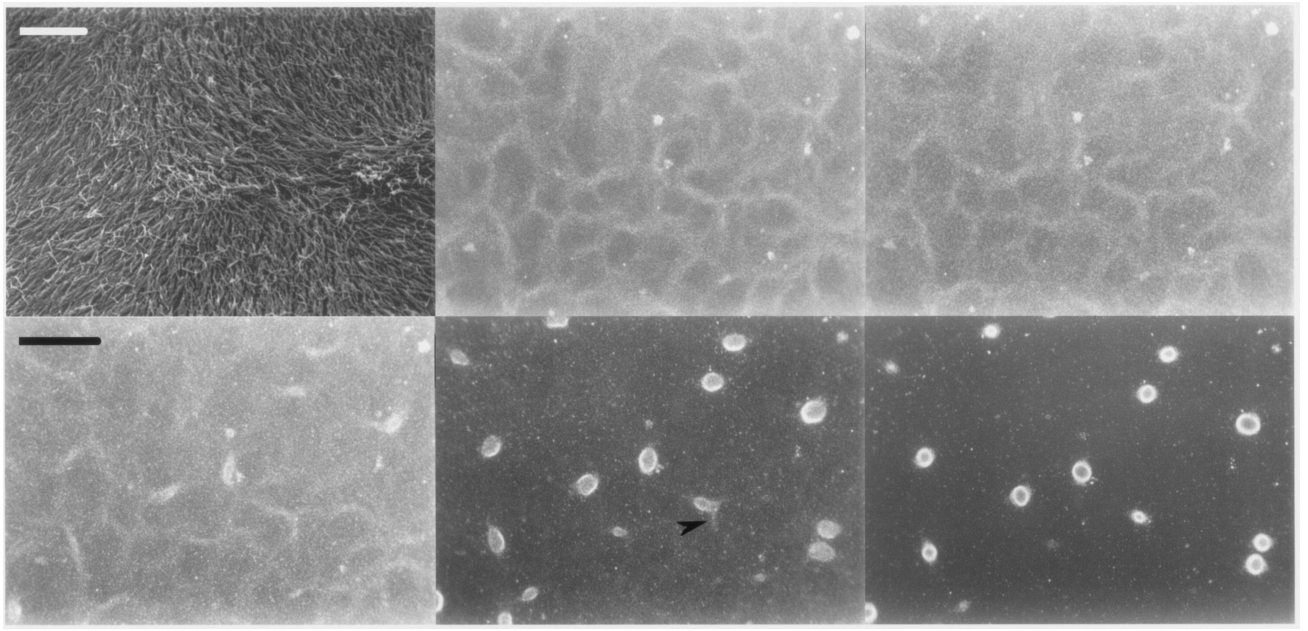

FIG. 1. Stages in the construction of fruiting bodies in submerged culture of Kuner type. Frames (top row): left frame, high-magnification scanning electron micrograph of the domain pattern in submerged culture (the image from reference 19; scale bar, 20 μm); middle frame, light microscopic image showing the network of ridges of the domain pattern at 1 h poststarvation (×6.3 objective lens, oblique illumination; for further details, see Materials and Methods); right frame, same field and technique as frame 2, photographed at 5 h. Frames (bottom row): left frame, same field at 8 h (scale bar, 1 mm); middle frame, same field at 11 h; right frame, same field at 24 h.

then to sporulate within it. We report here two new movement patterns that help to construct its fruiting bodies.

MATERIALS AND METHODS

Submerged culture on glass. The procedure is modified after that of Kuner and Kaiser (19). First, 2 ml of an exponential culture of DK1622 in Casitone-Tris medium (CTT), at a density of 2.5 Klett units, was added to a 2.5-cm diameter Corning Bionique culture dish with a metal baseplate, a Teflon core, and a Teflon gasket, with a microscope coverslip forming the bottom of the dish. After the culture had grown for 20 h at 31°C without agitation, the CTT fluid was removed by aspiration; the culture was next washed once with 3 ml of H_2O, which was replaced with 10 mM morpholinepropanesulfonic acid–1 mM $CaCl_2$, and then the culture was returned to 31°C to starve and to complete fruiting body development. A diagram of the setup is Fig. 3A. At the times indicated, the cultures were mounted on a mechanical stage of a Leitz Labovert inverted microscope to preset X and Y coordinates, with the dish coverslip directly above the objective lens at room temperature. The dish was photographed and then returned to the incubator. Specimens were photographed by using a phase contrast stop in the condenser to provide oblique illumination.

SAC. Two sterile 0.5-mm-thick silicone rubber gaskets (Grace Biolabs, Bend, Oreg.) were placed on top of a flame-sterilized glass microscope slide, creating a small well whose bottom half was filled with 1.5% agar in clone-fruiting (CF) medium. After the agar hardened, the *M. xanthus* culture was spotted onto it and allowed to dry for 5 min, and then the well created by the second gasket was filled with CF liquid medium. The final layers of a submerged agar culture (SAC) apparatus consisted of the coverslip, a gasket containing CF liquid, a gasket containing agar, and a slide. The *M. xanthus* population is between the agar and the CF liquid. A diagram of the setup is shown in Fig. 3B, and additional details are given in Fig. 1 of reference 39).

SAC cultures were maintained at 25°C with a heated stage (Brook, Lake Villa, Ill.) for the acquisition of time-lapse images. Video microscopy was performed on a Nikon Eclipse E800 microscope (Nikon, Melville, N.Y.) by using long working distance objectives. Digital images were acquired from an analog video source by using a Scion LG-3 video capture card and Scion Image software (Scion, Frederick, Md.). Phase-contrast images were generated with a charge-coupled device camera (Optronics Engineering, Goleta, Calif.). Images were saved at regular intervals (either 20 or 60 s per frame), and background noise was reduced by averaging the video rate images over a period of 2 s. Images were saved as sequentially numbered TIFF files and assembled into time-lapse movies by using Quicktime (Apple Computer, Cupertino, Calif.).

RESULTS

Morphological stages in aggregation. As *Myxococcus* cells settle from suspension onto the glass floor of a submerged culture dish and grow beneath the CTT liquid medium to confluence, they also move to form plate-like multicellular domains (19). These domains range from 0.2 to 0.4 mm in diameter, and in each the rod-shaped cells lay side by side with their long axes roughly parallel, as can be seen in the scanning electron micrograph of Fig. 1, frame 1. Where two adjacent domains intersect, the difference in their cell orientation prevents a smooth abutment, and a slightly elevated ridge is formed. An intersection of four domains and their ridges is evident in the upper right quadrant of frame 1. A light microscope image taken with a ×6.3 objective lens under oblique illumination (Fig. 1, frame 2) of a submerged culture 1 h after the replacement of CTT (growth) medium with morpholinepropanesulfonic acid-Ca starvation buffer to start development emphasizes the ridges because they scatter more light than the plate-like domains. With the help of a mechanical stage equipped with a vernier scale, the specimen was repositioned with a (measured) accuracy of ±5 μm, the average length of one cell. In this way, the very same microscopic field was photographed at 1, 5, 8, 11, and 24 h to show how the cell arrangement changes as fruiting bodies develop. To obtain a significant sample of the culture, eight different microscope fields were photographed at these time points. A representa-

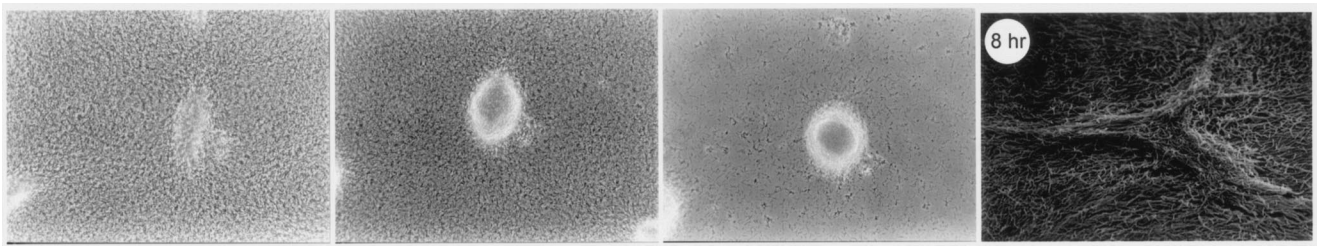

FIG. 2. Stages in fruiting body aggregation in Kuner submerged culture. A single field was photographed at 8, 11, and 24 h for the first three frames. Conditions were as described for Fig. 1, except the photographs were taken with a ×16 phase-contrast objective. The last frame (8 h) shows an electron micrograph of an early aggregate from reference 19.

tive field is illustrated in Fig. 1, frames 2, 3, 4, 5, and 6, which show successive time points.

The other seven fields showed the same type of changes over time as those in Fig. 1, and a description of the features general to all eight cultures follows. At 5 and 8 h, the original network of ridges has generally faded; then, especially clearly at 8 h, a few of the original elements became brighter (Fig. 1, frames 3 and 4). Higher-magnification views showed no pale cells, cell fragments, or other signs of cell lysis at 8 h (see, for example, Fig. 2). For that reason, the fading and brightening implies that cells are collecting at certain points. The bright elements of the network at 8 h appeared smaller and higher in cell density than the ridges at 1 h, implying that the bright elements are condensations. These condensates at 8 h are also asymmetric, with tails that lead in several directions away from their centers. Some tails are still evident at 11 h; one is indicated with an arrow in Fig. 1, frame 5. One such condensate is, shown in the Fig. 2, 8-h photo. That scanning electron photomicrograph shows an elongated asymmetric heap of cells whose long axis is 80 μm and short axis 15 μm, which can be seen to contain many hundreds of cells (19). Viewed by phase-contrast light microscopy, one 8-h elongated heap and parts of two others are evident in the middle of Fig. 2, frame 1, and at the edges of that field.

Since precisely the same field was photographed from 1 to 24 h, it was possible to superimpose the 8-h photos onto the corresponding 1-h photos of Fig. 1 and of the other culture fields (not in the figure). Superimposition revealed that all of these elongated heaps had been constructed on a ridge of the 1-h network. Moreover, the tails of these 8-h aggregates superimposed on other ridges that had branched from the first in the 1-h network. By 11 h, some of these asymmetric aggregates enlarge and round up, while others fade (compare Fig. 1, frames 4 and 5). It is as if the rounded aggregates have drawn in cells from the space between aggregates because the tails (arrow in frame 5) have vanished as the aggregate rounds up (frame 6), and fewer cells are evident between aggregates (Fig. 1 and 2). By 24 h, there are very few cells outside the rounded aggregates, as shown by the paucity of points that scatter light in the field outside them (Fig. 1 and 2).

As mentioned, superimposition of the 24-h photos onto the earlier photos showed that all of the nascent fruiting body aggregates arose from asymmetric aggregates at 8 h, which in turn arose from elements of the 1-h network of ridges. However, only certain elements of the original network nucleated a fruiting body. Considering the 1-h ridge pattern as an irregular network that covers the surface (diagrammed in Fig. 3C), three classes of geometric objects were distinguished: a face, i.e., a single domain surrounded by edges, an edge where two domains overlap, and vertices where three domains intersect. Point-to-point superimposition was made on 43 nascent fruiting bodies, and 36 of these tracings could be completed without ambiguity. (There was ambiguity when a ridge was so broad that the adjacent facets were difficult to discern.) According to the 36 unambiguous traces, none of the fruiting bodies arose from a face, 34 arose from an edge, and 2 may have arisen from an edge or possibly a vertex (because the ridges at the vertex were broad). Thus, 36 fruiting bodies could be traced back to a ridge in the initial domain pattern. In every case, the long axis of the asymmetric aggregates at 8 h corresponded to the orientation of the ridge in the domain pattern. The field in Fig. 1, frame 2, initially had 133 ridges that produced 13 fruiting bodies. Thus, a small fraction of ridges give rise to a fruiting body.

Kuner and Kaiser (19) showed that fruiting bodies in submerged culture, such as those in Fig. 1, frame 6, and older contain viable, heat-resistant spores. Sporulation in submerged culture has been amply confirmed in other studies (33, 34).

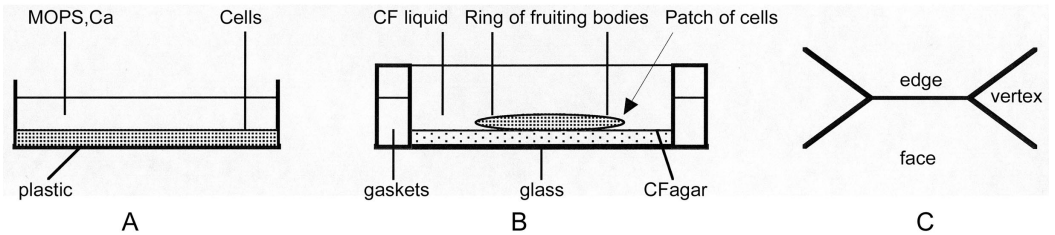

FIG. 3. Diagrams showing the setup of the two types of submerged culture used in the present study and the network. (A) Previously described conditions (19). The cells are in contact with glass. In the text, this is referred to as Kuner culture. (B) SAC conditions described previously (39). The cells rest on CF agar. In the text, this is referred to as SAC. (C) Diagrammatic definitions of edge, face, and vertex.

Sporulation is the last step in fruiting body development, and it takes place even when fruiting bodies are submerged. The same fields viewed in Fig. 1 were also photographed at ×16 in phase contrast to view individual cells. Figure 2, frame 1, shows that most of the cells between the 8-h asymmetric aggregates and the 11-h symmetric aggregates have disappeared by 24 h, when sporulation has commenced. Julien et al. showed that peripheral cells are not expressing C-signal-dependent genes and, for that reason, are unable to sporulate (14). Cells located between different aggregates at 11 and 24 h are likely to be the peripheral rods described by O'Connor and Zusman (22). The 24-h image in Fig. 2 (frame 3) and those photographed at ×16 at five other sites (not shown) suggest that peripheral rods in submerged culture would eventually lyse.

To check whether fruiting bodies are clustered in submerged culture, their spatial distribution was analyzed. Thirty-four photographs, like Fig. 1, frame 6, and containing a total of 653 fruiting bodies, were randomly sampled by using a square of fixed size. The size of the sampling square was such that about one fruiting body would be obtained per sample. As it turned out, the average number of fruiting bodies per sample square ranged from 0.28 to 2.1 over all 34 photos. For each photograph, the number of sample squares that captured no fruiting bodies, those with 1, 2, or ≥3 fruiting bodies, the total number of fruiting bodies captured in the samples, and the total number of samples were recorded. If, on the one hand, the spatial distribution were very orderly, the numbers of fruiting bodies per sample are expected to be mostly 1's, a few 2's, a few 0's, and probably no 3's. On the other hand, if fruiting bodies were independently distributed, then the numbers of samples with 0, 1, 2, or ≥3 fruiting bodies would have Poisson statistics. The proper Poisson distribution would be set by the average number of fruiting bodies per unit area for each photograph. Table 1 shows χ^2 tests of the hypothesis that the data are described by the Poisson distribution appropriate for each of the 34 photographs (1). The level of significance is too high for all plates to reject the hypothesis that fruiting bodies are distributed independently. Complete independence might not be expected if nascent aggregates that form close to one another often fuse, as is observed in the agar cultures described below. Such fusion would create a deficiency of samples with two or more fruiting bodies and a corresponding excess of samples with none. Keeping the possibility of fusions in mind, the distribution of fruiting bodies is consistent with independent sites of aggregation on the 0-h network of ridges.

Based on fruiting body locations, at least two steps can be discerned at which the sites of mature fruiting bodies are determined. The first is the selection of a ridge to become an asymmetric aggregate. Of the 133 edges in Fig. 1, frame 2, 22 bear an aggregate at 8 h. The second step is the selection of an asymmetric aggregate to enlarge into a symmetric fruiting body; of the 22 fruiting bodies marked at 8 h, 13 remained at 24 h. The number of different microscopic cell arrangements in a culture of $\sim 10^8$ cells would be very large, as the field shown in Fig. 2, frame 1, makes plain. In Fig. 2 and the other photos (not shown), no repeating structures, apart from the aggregates themselves, were apparent. Rather, the independence of fruiting body sites is consistent with determination by the unique microarrangements of cells, any one of which has a very low probablility of nucleating an aggregate.

TABLE 1. Spatial distribution of fruiting bodies (fb) in submerged culture

Plate no.	Spatial distribution (no.)[a]				Mean no.	% Confidence[b]
	0 FB	1 FB	2 FB	≥3 FB		
1	2	5	2	0	1.00	70
2	19	21	1	1	0.62	92
3	4	2	3	0	0.78	99
4	2	4	3	1	1.30	94
5	25	10	1	0	1.33	90
6	2	4	2	1	1.33	90
7	15	23	4	0	0.74	96
8	16	22	4	0	0.71	98
9	16	20	6	0	0.76	99
10	16	20	6	0	0.76	99
11	14	20	8	0	0.86	98
12	24	16	2	0	0.48	99
13	27	13	2	0	0.40	99
14	21	19	2	0	0.55	99
15	21	18	3	0	0.57	99
16	20	22	0	0	0.52	98
17	24	16	2	0	0.48	99
18	21	19	2	0	0.55	99
19	22	19	1	0	0.50	99
20	1	5	2	1	1.33	80
21	22	20	0	0	0.48	98
22	18	22	1	1	0.64	98
23	27	13	2	0	0.40	99
24	22	18	2	0	0.52	99
25	25	16	1	0	0.43	99
26	1	5	3	0	1.22	70
27	2	3	3	1	1.22	80
28	1	7	1	0	1.00	60
29	0	6	1	2	1.44	70
30	1	2	4	2	2.00	50
31	0	4	4	1	1.67	40
32	0	5	4	0	1.44	40
33	0	4	2	3	1.89	50
34	1	1	4	3	2.10	30

[a] FB, fruiting body.
[b] That is, the level of confidence calculated from the χ^2 distribution (1) that the spatial distribution is Poisson.

Morphogenesis in SAC. Fruiting body development in SAC has been photographed in time lapse by Welch, originally for the purpose of tracking cells in traveling waves (39). Beyond the waves, Welch's photographs documented the patterns of cell movement during aggregation in detail. A frame-by-frame analysis of the movie revealed the early formation of stationary aggregates, similar in their temporary immobility (for many hours) to the asymmetric aggregates described above in Kuner submerged culture. The Welch movies also show interactions between traveling waves and the stationary aggregates. Finally, the Welch photos show how stationary aggregates subsequently move. Welch's submerged cultures differ in three ways from those photographed for Fig. 1 and 2 (see diagram in Fig. 3). First, the cells are moving and aggregating on a thin layer of agar in CF medium rather than on the glass surface of a microscope coverslip in buffer in A. Second, all of the fruiting bodies form along the perimeter of the initial inoculum of cells in SAC (Fig. 3B) because there is a physical barrier, probably surface tension, to outward movement of cells at the edge (39). In Fig. 3A, fruiting bodies formed at spatially random locations all over the glass substrate. Finally, traveling waves are strong in the setup of Fig. 3B, whereas they are not observed in

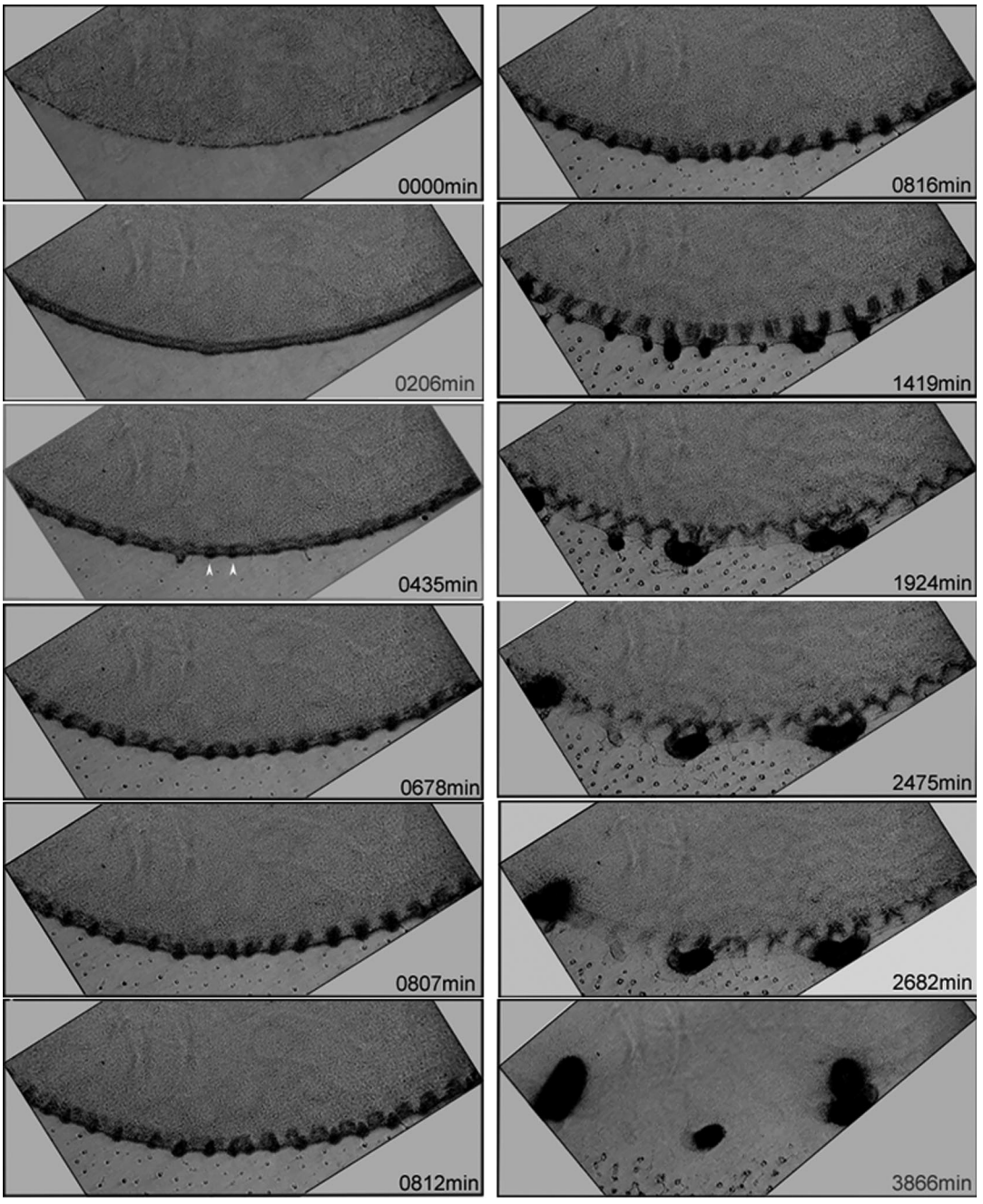

FIG. 4. Stages in the construction of fruiting bodies in SAC. The edge of an SAC, as diagrammed in Fig. 3B, is shown at the times indicated. Individual frames taken from a time-lapse movie (download from http://cmgm.stanford.edu/devbio/kaiserlab/) were rotated to bring the edge into a horizontal position. Lapsed time is shown in the lower right corner of each frame. Each frame is the same microscopic field; therefore, the vertical lines drawn through the column of frames cross the edge of each frame at the same position. White arrows in the 435-min frame indicate the two arc-shaped zones discussed in the text.

cultures of the Fig. 3A type. This indicates that movement is generally more organized in the Fig. 3B condition. Despite these differences, the cultures depicted in Fig. 3A and B show the same two stages: fixed aggregate formation that is followed by selective enlargement of certain aggregates. With a photograph taken every 1.5 min, the Fig. 3B cultures offer greater time resolution and more structural detail than those of Fig. 3A, in which photographs were taken at 3- to 5-h intervals.

A time-lapse movie of *M. xanthus* fruiting body development can be downloaded from http://cmgm.stanford.edu/devbio/kaiserlab/.

Starting from a uniform cell density across the culture at 0 min (Fig. 4), cells swarm outward from the center of the culture, first accumulating to form a band of elevated cell density around the original edge of the culture. Cells within that band tend to be oriented parallel to the edge, as described previously

(39). Initially, the band appears uniformly dark around its circumference, as shown in Fig. 4 (206 min). Then, ca. 140 min later, density variations can be perceived when two lumpy sets of cells appear to travel around the band: one set moving clockwise and the other set moving counterclockwise. At their start, these lumps are evident in the time-lapse video, but they are not resolved in a single still photograph. Shortly, however (Fig. 4, 435 min), dark, arc-shaped zones are evident at the outer edge of the band in the still photographs, each arising from the outer edge of a lump. Two such arcs are indicated by white arrows in the 435-min frame, and others are evident but are not labeled. Even though the arcs appear to have arisen from moving lumps, these arcs are stationary; they can be recognized later at the same position through at least 812 min. At 435 min the inner edge of the band directly opposite an arc was a moving lump of optical density. After 435 min, the stationary arcs widen across the band toward its inner edge (Fig. 4, 678 min). As the arc spreads across the band, the arc becomes an elongated teardrop, whose point aims toward the center of the culture spot (located vertically above the top of Fig. 4 [678 min]).

Recall that the cells within the peripheral band have their long axes oriented tangent to the culture edge (39). By 678 min, the moving lumps of these cells have now sharpened into tangentially directed moving ridges, the crests of traveling waves, as a consequence of the focusing action described by Igoshin et al. (10). By 678 min, the lumps have become a clockwise and a counterclockwise set of traveling waves, moving around the band (Fig. 4) (39). The ridges of these waves make acute angles with the edge, and it becomes apparent that the tear-shaped fixed aggregates are regularly spaced at wavelength intervals in Fig. 4 (678 min). At that time, 18 aggregates could be distinguished, reading from left to right, and these were named A1 to A18.

The moving waves appear to wash over these 18 aggregates, whereas the latter remain fixed at their position. At this time the opacity of a wave crest is comparable to the opacity of an aggregate. As a consequence, the total opacity at the position of an aggregate fluctuates periodically as the waves move over it. For example, aggregate A12 was clocked over several cycles, and it has a period of six to seven movie frames of 1.5 min each. If the start of a cycle is taken when a wave crest coincides with the center of an aggregate, then the space between adjacent fixed aggregates at the start has a low optical density. The density of the aggregate plus the wave crest extends across the width of the band (Fig. 4, 807 min). Shortly thereafter (812 min), the wave crest is 180° out of phase with the aggregates, and the space between aggregates is darkened by a relatively broad and diffuse distribution of cells in the wave. It can be seen at 812 min that many cells remain stationary because none of the aggregates move; the waves move. In Fig. 4, 812 min, the waves are very plain between aggregates A12, A13, A14, A15, and A16. As the waves travel, they progress to the next set of registrations with aggregates at 816 min in Fig. 4. Cycling is readily observed if the movie is stepped from frame B17951 to frame B17957, one frame per step.

After many waves have washed, so to speak, over the aggregates, they can be seen to have grown larger. By comparing each aggregate in Fig. 4 at 816 min with its initial arc at 435 min, one can appreciate the growth. In the interval from 435 to 816 min, the center of each aggregate remains at the same position along the edge, showing no detectable lateral movement. This symmetrical growth of the aggregates suggests that some wave cells have been added to the aggregates. It also suggests that the new cells have not inserted into the asymmetric core of the aggregate but rather encircle the core. Many cells along the crest of a wave might cross an aggregate at about the same time, offering many opportunities to be deposited. A reverse process is also observed. Some aggregates dissipate, losing their density as waves wash over them; it is as if cells can leave an aggregate to rejoin the wave system. A3, A4, A9, A10, A11, A15, A16, A17, and A18 disappear with time; none of them are opaque at 1,419 min in Fig. 4.

Returning to 678 min, a few clumps of cells can be seen as dots beyond the edge of the original culture. (They appear below that edge in Fig. 4.) Before their appearance, no cells had been observed to migrate away from the edge into the area where the dots are found. The dots were not apparent at 0 min; they became visible at 206 min. Individual cells are too small to be seen at the magnification used for the movie, but after 206 min there will have been time for cells to aggregate into these now-visible clumps. Because these cells are few, they were not tracked. Suffice it to say that their capacity to enlarge by fusing with each other indicates that these are clumps of motile cells. At least three of them close to the perimeter of the culture spot were observed to fuse with an aggregate by means of thin, slime-like ribbons at 816 min.

The period of stationary aggregate dissipation and growth comes to an end when some aggregates are seen to move. In every case, adjacent aggregates fused with one another, joining at the pair's center of mass. In Fig. 4, 1,419 min, A12 and A13 are seen to be moving and fusing. Then, at 1,924 min, A7 and A8 fuse. Later, fused aggregates are observed to fuse with another. Again, it is always adjacent aggregates that fuse. Eventually, only three large aggregates remain in this sector of the culture to become fruiting bodies in Fig. 4, 3,866 min; originally there had been 18 stationary aggregates. Secondary fusion shows that one fusion does not exhaust the capacity of a motile aggregate to fuse, and these properties suggest a mechanism of fusion described in the Discussion.

Just as small aggregates fuse with each other, A5 fuses with the wave system. This later fusion of an aggregate with the waves differs from the loss of cells from an early nonmotile aggregate back to the waves described above in that A5 is motile. First, A5 bends to the right, taking up an orientation that confronts the waves, then the interior of A5 flows rapidly toward a wave. This flow suggests that most cells within a motile aggregate are streaming (15). Initially, the flow leaves behind a thin, U-shaped, empty shell (Fig. 4, 2,475 min). Finally, and more slowly, the shell also dissipates, giving up almost all its density to the wave system (Fig. 4, 2,682 min). In addition, the left part of the fused A7 and A8 at 3,866 min becomes another shell, apparently by fusion with waves.

Moving waves are still evident at 2,682 min. However, their optical density has fallen because the waves may have suffered a net loss of cells to the growing, motile aggregates. The waves may also have gained cells from the center of the culture spot due to outward swarming. Nevertheless, the wavelength changed little from 678 to 2,682 min. Since the wavelength is expected to depend on the cell density in the wave crests (10),

TABLE 2. Tracks of cells near aggregates[a]

Movie	No. of cells:		No. of aggregates	Fraction of total surface
	Coincident with an aggregate	Off the surface of any aggregate		
M1	7	7	2	0.07
M2	9	5	2	0.21
M3	16	10	5	0.17
M4	9	5	4	0.16
Total	41	27	13	0.15

[a] All four movies were recorded after 15 h of development in cell patches on 2-mm-thick A50-agarose (9) slabs (1.5% agarose). Individual frames were recorded with 15-s intervals over a period of 15 min (60 frames in all). All of the movies contain DK1622 mixed with GFP-conjugated DK1622 at a ratio of 300:1.

the crest density appears to have remained high. This could be explained by the focusing effects. In any case by 3,866 min, the waves are no longer visible. All visible cells are concentrated in the three large aggregates evident in Fig. 4. All three pulse for a short time at approximately the frequency of the traveling waves. Although pulsing is not evident in a still image, it is quite marked in movie frames B19820 to B19980 (http://cmgm.stanford.edu/devbio/kaiserlab/).

Cell movement in the vicinity of enlarging aggregates. In mixtures of a few fluorescent (i.e., green fluorescent protein-labeled) *M. xanthus* cells and many nonfluorescent cells, individual fluorescent cells can be tracked even in regions of high total cell density. Using a ratio of 1 fluorescent/300 nonfluorescent cells, L. Jelsbak has made several time-lapse movies of cells moving in the vicinity of fruiting body aggregates that are enlarging on the surface of a slab of agarose (L. Jelsbak, unpublished results). Jelsbak photographed at 15 h of development before sporulation had begun, and he has made these images available to us for cell tracking. Table 2 shows data from four of Jelsbak's movies with a total of 13 aggregates, all nonfluorescent, and 68 fluorescent cells. During the 15-min movies, some of the 68 tracked cells appeared for all or part of their trajectories to coincide with an aggregate, as if they were moving from the adjacent less-organized mass of cells onto the top surface of an aggregate. Since the photographs were taken from the top of the culture downward, these fluorescent cells must be in contact with the top surface of the aggregate. Other fluorescent cells in the same microscopic field never coincided with an aggregate during their 15-min period of photography and presumably are near the top of the surrounding mat of cells at lower density because they are less well organized. Table 2 shows the number of fluorescent cells coincident with the dense image of an aggregate at some point in their trajectory, the number never coincident, and the fraction of the microscopic field's area that is occupied by its aggregates. For the spatial distribution of fluorescent cells, the data of Table 2 shows that, although aggregates accounted for only 15% of the average area of the frames, 60% of the fluorescent cells were coincident with an aggregate. Since the coincident cells are bright and moving, they are not within the aggregate, adhering to it, or trying to penetrate it. The bias favoring coincidence suggests that cells approaching an aggregate from the neighborhood may turn to glide on the aggregate's surface and may be trapped there for a while. These cells may be contributing to the enlargement of an early aggregate, as reported above for Kuner submerged cultures and for SAC.

DISCUSSION

The data on cell movement and on changes in the shape and size of aggregates reported here give evidence of two new steps in aggregation. The first step is the formation of stationary clusters of cells; they were observed in both Kuner submerged culture and in SAC. In SAC, 18 such clusters were observed to form simultaneously, spaced one ripple wavelength apart along the culture edge (Fig. 4). Every pair of countermigrating wave crests initiated an aggregate. The location and regular spacing of those aggregates suggests the following mechanism. At the time, the edge is a band of relatively high cell density; the traveling waves are evident as "lumps" of cell density. Although obscure in still images, the moving lumps can be perceived at movie speed (http://cmgm.stanford.edu/devbio/kaiserlab/). A regular spacing of one wavelength suggests that the aggregates form at intersections of a rightward-moving wave, a left-moving wave, and the high-density edge of the peripheral band, as diagrammed in Fig. 5. There would be more cells at such intersections than anywhere else. Cells in a wave are moving when they arrive at the intersection, and band cells may also be moving though with less regularity. Both A and S motilities are known to be required for traveling waves (32). Moving cells might stop at the triple intersections, because, like so many motor cars arriving on roads from several opposite directions, the cells find themselves stuck in a traffic jam that inhibits each other's movement. Worse than cars on flat roads, cells could enter their jam from outside the plane, and the cell jams would

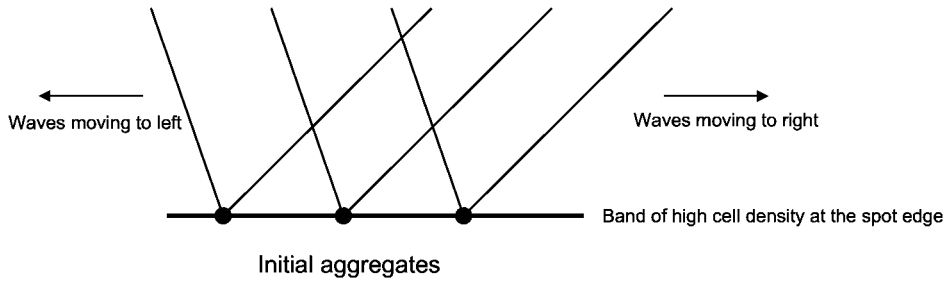

FIG. 5. Explanation for the position and regular spacing of the initial aggregates in submerged agar culture. It is proposed that stationary aggregates form at triple intersections, as shown, between the crest of a left-moving wave, the crest of a right-moving wave, and the annular band of high cell density at the spot edge. These intersections create a traffic jam.

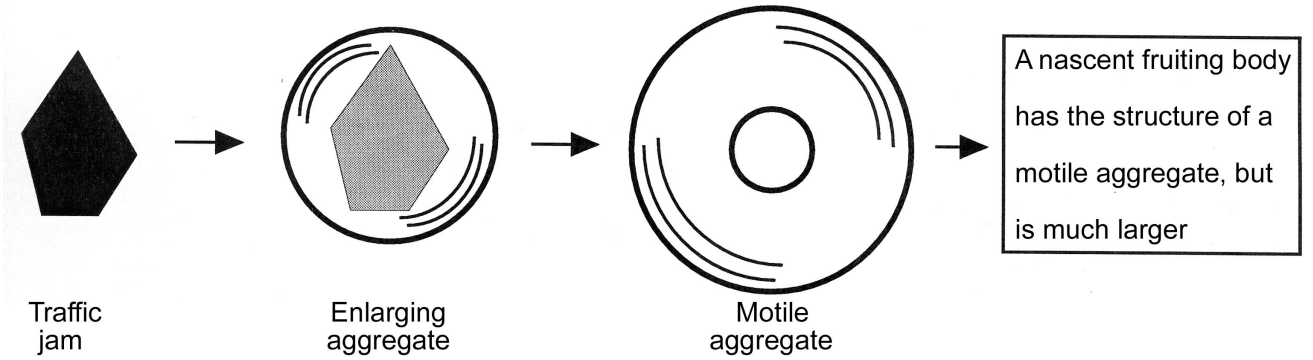

FIG. 6. Model for aggregation and fruiting body development. The model combines observations in Kuner submerged culture and SAC and is explained in the text. Although the aggregates are solid bodies, for simplicity they are represented by their average cross-sections, as if viewed from above. The traffic jam from Kuner cultures is represented as an asymmetric polygon (see Fig. 2, 8 h; they are arc-shaped in SAC [Fig. 4, 435 min]).

be three-dimensional. Mechanically, both engines would be expected to stall if a cell's forward motion were blocked by other cells. Wolgemuth et al. have detailed that argument for the force generated by the A-engine (41), and S motility could also be blocked by a barricade. Like traffic jams, the aggregates remain stationary for more than 6 h in SAC.

Aggregates also formed at sites where cells had piled up in Kuner submerged cultures. At these sites, two plate-like domains of cells, each with a different cell orientation and thus out of register with each other and overlapping, are located. Kuner aggregates are asymmetric and elongated along the edge where two domains overlap (Fig. 1 and 2). However, only a fraction of the edges nucleate an aggregate because each has a unique microarrangement of cells according to the history of how that arrangement came about. As *M. xanthus* glides, the cell leaves a trail of slime, and that trail guides other cells that happen to cross it (5, 15, 41). The trails are not observable in confluent cultures such as are shown in Fig. 1 and 2, but they do constrain the future movements of each cell and thus its potential for aggregation. The scanning electron micrograph image of one such aggregate has the appearance of a flattened traffic jam (see Fig. 2, 8 h). No traveling waves were observed in these cultures, and the aggregates remained stationary from 8 h to 24 h. However, during these 16 h the aggregates grew in size and gained circular symmetry. It is as if their cells were orbiting around. Indeed, cells were observed to turn and to glide on the surface of an aggregate (Table 2), and cells at the base of such aggregates have been tracked in circular orbits, as shown by Sager and Kaiser (see Fig. 6 in reference 31). Cell vortex patterns have been observed in scanning electron micrographs of nascent fruiting bodies (24).

After they enlarged for about 6 h, the stationary aggregates in SAC began to fuse with each other. A model, based on the observations described above, for the conversion of a stationary traffic jam into a motile aggregate is presented in Fig. 6. The gradual loss of density in the waves and concurrent gain in density of the aggregates from 435 min to 3,866 min (the movie or Fig. 4) suggest that there is net transfer of cells from wave crests to enlarging aggregates. We suggest that the transferred cells circulate in orbits around a core consisting of a stationary traffic jam, enlarging and rounding the aggregates. That circulation is represented by thin arcs within the aggregates in Fig. 6. The ability of motile aggregates to fuse with each other clearly shows that their constituent cells are moving. The organization of that movement is suggested by other experiments in which equal numbers of cells were found by tracking to be circulating clockwise and counterclockwise in the nascent fruiting bodies (31). No reversals were observed in experiments of tracks within an aggregate; however, reversals were observed in cells outside the aggregate (31).

M. xanthus cells are flexible because their peptidoglycan is organized as articulating plates (4). The long and flexible myxobacterial cells would be expected to bend and turn at a barrier if they were being pushed by slime secretion from their rear (41). Moreover, the movies of Reichenbach and Kuhlwein show cells turning after collision with another cell (18). Finally, the tracking data of Table 2 suggest that, when cells encounter a dense aggregate, they turn and move along its surface. As a result of their capacity to turn, stalled cells within the traffic jam core of an enlarging aggregate would begin to navigate around the cells within the jam that block their forward progress, either by turning as just described or by reversing at each blockade. These movements that would break the jam are represented in Fig. 6 by the lighter gray of the core in an enlarging aggregate than in the traffic jam. According to the model, an aggregate would become motile and capable of fusion only after all of the cells of the traffic jam had begun to circulate, as in the motile aggregate represented in Fig. 6. The central hole shown in the motile aggregate was observed by Sager as a region of low cell density (31). Two such motile aggregates would be expected to have the ability to fuse with one another, creating one larger circulation that retained the capacity to fuse again. Indeed, serial fusion is observed in SAC between 816 min and 3,866 min (see movie and Fig. 4).

Several consecutive fusions result in an aggregate of fruiting body size (as evident in the movie from 1,419 to 3,866 min and Fig. 4). Other experiments have shown that many cells circulating within an aggregate the size of a fruiting body transmit C signal to each other as they stream at high cell density (11, 12, 15). Repeated C signaling between cells within a nascent fruiting body aggregate would be expected to raise the level of C signal on cells, via the *act* positive feedback loop, up to the threshold for sporulation (6, 7). Finally, myxospore differentiation would be induced (15, 35).

The model of Fig. 6 combines the structural data from two types of submerged culture. Cell movement is more highly organized in SAC (Fig. 3B) than in Kuner cultures (Fig. 3A): Kuner fruiting bodies arise randomly on the lawn of cells (Table 1), whereas in SAC aggregates are initiated at one-wavelength intervals around the edge of the lawn or patch of cells (Fig. 5). Despite a difference in initial organization, the aggregates at 11 h in Kuner submerged culture (Fig. 1 and 2) have the same rounded shape and about the same size as the mounds in SAC, suggesting that cells in the Kuner fruiting bodies are circulating in the same way as those in SAC. Since traffic jams and circulating cells are observed in both types of submerged cultures, we suggest that these two structures are likely to be used in the formation of fruiting bodies under other conditions, including within a patch of cells that is open to the air (40). Because the sites of fruiting body formation in open agar plate cultures are unpredictable, we have been unable to trace enlarging aggregates backward in time to their initiating aggregate, as we have done in SAC (Fig. 4). The experiments in Kuner submerged culture and SAC predict that the initial aggregates will be a kind of traffic jam, and Jelsbak and Søgaard-Andersen recently reported small jam-like clusters of fluorescent cells on agar plate cultures (see Fig. 2 [6 h] in reference 13).

ACKNOWLEDGMENTS

This study was supported by Public Health Service grant GM23441 to D.K. and by postdoctoral fellowship GM20356 to R.W. (both from the National Institute of General Medical Sciences).

Brooke Danaher expertly tracked cells in the Welch and Jelsbak movies. We thank L. Jelsbak for access to four of his movies. O. Igoshin, G. Oster, and M. Alber contributed helpful suggestions.

REFERENCES

1. **Bevington, P. R.** 1969. Data reduction and error analysis for the physical sciences. McGraw-Hill Book Co., New York, N.Y.
2. **Blackhart, B. D., and D. Zusman.** 1985. The frizzy genes of *Myxococcus xanthus* control directional movement of gliding motility. Proc. Natl. Acad. Sci. USA **82:**8767–8770.
3. **Burchard, R. P.** 1970. Gliding motility mutants of *Myxococcus xanthus.* J. Bacteriol. **104:**940–947.
4. **Dworkin, M.** 1993. Cell surfaces and appendages, p. 77. *In* M. Dworkin and D. Kaiser (ed.), Myxobacteria II. ASM Press, Washington, D.C.
5. **Fontes, M., and D. Kaiser.** 1999. *Myxococcus* cells respond to elastic forces in their substrate. Proc. Natl. Acad. Sci. USA **96:**8052–8057.
6. **Gronewold, T. M. A., and D. Kaiser.** 2001. The *act* operon controls the level and time of C-signal production for *Myxococcus xanthus* development. Mol. Microbiol. **40:**744–756.
7. **Gronewold, T. M. A., and D. Kaiser.** 2002. *act* operon control of developmental gene expression in *Myxococcus xanthus.* J. Bacteriol. **184:**1172–1179.
8. **Harris, B. Z., D. Kaiser, and M. Singer.** 1998. The guanosine nucleotide (p)ppGpp initiates development and A-factor production in *Myxococcus xanthus.* Genes Dev. **12:**1022–1035.
9. **Hodgkin, J., and D. Kaiser.** 1979. Genetics of gliding motility in *M. xanthus* (*Myxobacterales*): two gene systems control movement. Mol. Gen. Genet. **171:**177–191.
10. **Igoshin, O., A. Mogilner, R. Welch, D. Kaiser, and G. Oster.** 2001. Pattern formation and traveling waves in myxobacteria: theory and modeling. Proc. Natl. Acad. Sci. USA **98:**14913–14918.
11. **Jelsbak, L., and L. Søgaard-Andersen.** 1999. The cell-surface associated C-signal induces behavioral changes in individual *M. xanthus* cells during fruiting body morphogenesis. Proc. Natl. Acad. Sci. USA **96:**5031–5036.
12. **Jelsbak, L., and L. Søgaard-Andersen.** 2002. Pattern formation by a cell-surface associated morphogen in *Myxococcus xanthus*. Proc. Natl. Acad. Sci. USA **99:**2032–2037.
13. **Jelsbak, L., and L. Søgaard-Andersen.** Cell behavior and cell-cell communication during fruiting body morphogenesis in *Myxococcus xanthus.* J. Microbiol. Methods, in press.
14. **Julien, B., A. D. Kaiser, and A. Garza.** 2000. Spatial control of cell differentiation in *Myxococcus xanthus.* Proc. Natl. Acad. Sci. USA **97:**9098–9103.
15. **Kaiser, D.** 2003. Coupling cell movement and multicellular development in *Myxobacteria.* Nat. Rev. Microbiol. **1:**45–54.
16. **Kaiser, D.** 1979. Social gliding is correlated with the presence of pili in *Myxococcus xanthus.* Proc. Natl. Acad. Sci. USA **76:**5952–5956.
17. **Kaiser, D., and C. Crosby.** 1983. Cell movement and its coordination in swarms of *Myxococcus xanthus.* Cell Motil. **3:**227–245.
18. **Kuhlwein, H., and H. Reichenbach.** 1968. Swarming and morphogenesis in myxobacteria. Film C893/1965. Institut Wissenschaftlichen Film, Gottingen, Germany.
19. **Kuner, J., and D. Kaiser.** 1982. Fruiting body morphogenesis in submerged cultures of *Myxococcus xanthus.* J. Bacteriol. **151:**458–461.
20. **Kuspa, A., L. Kroos, and D. Kaiser.** 1986. Intercellular signaling is required for developmental gene expression in *Myxococcus xanthus.* Dev. Biol. **117:** 267–276.
21. **Nudleman, E., and D. Kaiser.** Pulling together with type IV pili. J. Mol. Microbiol. Bio/Technol., in press.
22. **O'Connor, K. A., and D. R. Zusman.** 1991. Behavior of peripheral rods and their role in the life cycle of *Myxococcus xanthus.* J. Bacteriol. **173:**3342–3355.
23. **O'Connor, K. A., and D. R. Zusman.** 1991. Development in *Myxococcus xanthus* involves differentiation into two cell types, peripheral rods and spores. J. Bacteriol. **173:**3318–3333.
24. **O'Connor, K. A., and D. R. Zusman.** 1989. Patterns of cellular interactions during fruiting-body formation in *Myxococcus xanthus.* J. Bacteriol. **171:** 6013–6024.
25. **Reichenbach, H.** 1993. Biology of the myxobacteria: ecology and taxonomy, p. 13–62. *In* M. Dworkin and D. Kaiser (ed.), Myxobacteria II. ASM Press, Washington, D.C.
26. **Reichenbach, H.** 1966. *Myxococcus* spp. (Myxobacterales) Schwarmentwicklung und Bildung von Protocysten. Institut Wissenschaftlichen Film, Gottingen, Germany.
27. **Reichenbach, H., H. H. Heunert, and H. Kuczka.** 1965. Archangium violaceum (Myxobacterales)-Schwarmentwicklung und Bildung von Protocysten. Film E777. Institut Wissenschaftlichen Film, Gottingen, Germany.
28. **Reichenbach, H., H. H. Heunert, and H. Kuczka.** 1965. Chondromyces apiculatus (Myxobacterales)-Schwarmentwicklung und Morphogenese. Film E779.Institut Wissenschaftlichen Film, Gottingen, Germany.
29. **Reichenbach, H., H. H. Heunert, and H. Kuczka.** 1965. Myxococcus spp. (Myxobacteriales) Schwarmentwicklung und Bildung von Protocysten. Film E778. Institut Wissenschaften Film, Gottingen, Germany.
30. **Sager, B., and D. Kaiser.** 1993. Spatial restriction of cellular differentiation. Genes Dev. **7:**1645–1653.
31. **Sager, B., and D. Kaiser.** 1993. Two cell-density domains within the *Myxococcus xanthus* fruiting body. Proc. Natl. Acad. Sci. USA **90:**3690–3694.
32. **Shimkets, L., and D. Kaiser.** 1982. Induction of coordinated movement of *Myxococcus xanthus* cells. J. Bacteriol. **152:**451–461.
33. **Shimkets, L., and D. Kaiser.** 1982. Murein components rescue developmental sporulation of *Myxococcus xanthus.* J. Bacteriol. **152:**462–470.
34. **Søgaard-Andersen, L., F. Slack, H. Kimsey, and D. Kaiser.** 1996. Intercellular C-signaling in *Myxococcus xanthus* involves a branched signal transduction pathway. Genes Dev. **10:**740–754.
35. **Søgaard-Andersen, L.** 2003. Coupling gene expression and multicellular morphogenesis during fruiting body formation in *Myxococcus xanthus.* Mol. Microbiol. **48:**1–8.
36. **Sproer, C., H. Reichenbach, and E. Stackebrandt.** 1999. Correlation between morphological and phylogenetic classification of myxobacteria. Int. J. Syst. Bacteriol. **49:**1255–1262.
37. **Stanier, R. Y.** 1942. Elasticotaxis in myxobacteria. J. Bacteriol. **44:**405–412.
38. **Wall, D., and D. Kaiser.** 1999. Type IV pili and cell motility. Mol. Microbiol. **32:**1–10.
39. **Welch, R., and D. Kaiser.** 2001. Cell behavior in traveling wave patterns of *myxobacteria.* Proc. Natl. Acad. Sci. USA **98:**14907–14912.
40. **Wireman, J., and M. Dworkin.** 1975. Morphogenesis and developmental interactions in the myxobacteria. Science **189:**516–523.
41. **Wolgemuth, C., E. Hoiczyk, D. Kaiser, and G. Oster.** 2002. How *myxobacteria* glide. Curr. Biol. **12:**1–20.